Journal of Mechanics in Medicine and Biology
Vol. 18, No. 6 (2018) 1850064 (13 pages)

DOI: 10.1142/S0219519418500641

BIOMECHANICAL RATIONALE FOR CHOICE OF CEMENT MANTLE THICKNESS AROUND A FEMORAL STEM

IEVGEN LEVADNYI*, JAN AWREJCEWICZ†, OLGA SZYMANOWSKA‡
and DARIUSZ GRZELCZYK§

Department of Automation, Biomechanics and Mechatronics
Lodz University of Technology, 1/15 Stefanowski Str., 90–924 Lodz, Poland
**evgenabaqus@gmail.com*
†*jan.awrejcewicz@p.lodz.pl*
‡*szymanowska.olga@gmail.com*
§*dariusz.grzelczyk@p.lodz.pl*

JOSÉ EDUARDO GUBAUA¶, JUCÉLIO TOMÁS PEREIRA‖
and GABRIELA WESSLING OENING DICATI**

Laboratory of Computational Solid Mechanics
Federal University of Paraná, Rua XV de Novembro, 1299 — Centro
Curitiba — PR, 80060-000, Brazil
¶*jose.gubaua@yahoo.com.br*
‖*jucelio.tomas@ufpr.br*
***gabyoening@hotmail.com*

Received 7 March 2017
Revised 2 March 2018
Accepted 26 July 2018
Published 13 September 2018

The change in mechanical properties of the femoral bone tissue surrounding hip endoprosthesis stems during the post-operative period is one of the causes of implant instability, and the mathematical description of this phenomenon is the subject of much research. In the present study, a model of bone adaptation, based on isotropic Stanford theory, is created for further computer investigation. The results of implementation of such a mathematical model are presented regarding the choice of cement mantle rational thickness in cemented hip arthroplasties. The results show that for cement mantle thicknesses ranging from 1–1.5 mm, a peak stress value in the proximal part of the mantle exceeds the limit of durability of bone cement. Moreover, results show that high reduction in the bone density of distal and proximal regions was observed in cases of cement mantle thicknesses varying from 1–3 mm. No significant changes in bone density of the abovementioned regions were obtained for 4 mm and 5 mm. The outcome of numerical investigations can be treated as valuable and will lead to the improvement of cemented hip replacement surgery results.

Keywords: Bone remodeling; proximal femur; cement mantle thickness.

*Corresponding author.

1. Introduction

From a structural point of view, bone tissue has innumerous interesting properties. First, its compression tensile strength is similar to that of steel. Due to its heterogenic microstructure, bone is three times lighter and 10 times more flexible than steel. Further, bone can change its properties in response to several factors such as external load, age, and gender.[1,2] The variation in bone properties over time is referred to as bone remodeling, the primary aim of which is to replace old and damaged tissue for that which is healthy and new.[3]

Bone tissue adaptation, for example, is observed when a prosthesis is installed in the bone. After installation, the implant may significantly influence load transmission to the host tissue, which can cause excessive bone resorption at the bone–tissue interface and lead to aseptic loosening or even bone failure and/or fracture. Namely, the loads originally carried by the bone are in such a case applied to the femoral prosthesis, which further transmits them to the tissue in a changed form. Bone tissue is strongly affected by implantation of a component, and it is very important to understand the constitutive and structural behavior of the tissue, in order to investigate the adaptation to the new environment and to identify the correct treatment for each individual.[2]

One of the techniques employed to fix implants into host bones, termed cemented fixation, implements the utilization of a biological cement. In this technique, a bone-cement-prosthesis interface is created, where the cement keeps the component inside the femoral cavity. According to Jordão *et al.*,[4] the loads applied to the interface are spread in an approximately uniform way. The cement mantle is inserted into the femoral cavity made by a surgeon and penetrates the porous structure of the bone, which provides rapid fixation of the prosthesis.

In order to ensure long-term correct functioning of the bone-cement-implant system, an appropriate thickness of cement mantle and correct positioning of the hip joint stem endoprosthesis in the medullary canal should be ensured. First, a thin cement mantle may contribute to cracking of the cement[5,6] which, in turn, may lead to aseptic loosening or bone density increases (cortical hypertrophy).[7] Moreover, in the case of thick cement mantle, the load is likely to be poorly transferred to the bone, which can lead to bone atrophy[8,9] and final bone density reduction (a process known as stress shielding).

Several models aiming to simulate bone behavior and the process of adaptation due to applied loads have already been developed.[1,3,10–15] Thus, bone adaptation after implantation of the cemented prosthesis can be analyzed using bone remodeling models coupled with the finite element method (FEM), which is one of the most powerful tools to solve engineering problems and allowing for the execution of extensive studies in a rapid and inexpensive way. The abovementioned topic has been already described in numerous studies.[2,11,16]

The present study aims to evaluate bone adaptation around the femoral component as well as to investigate the effect that cement mantle thickness has on load

transfer to the host tissue. The objective is to make it possible to avoid fatigue fracture of the cement and provide even stress distribution in the bone, which, in turn, will allow treatment result improvements and increases in prosthesis durability. For this purpose, the FEM was implemented with the use of ABAQUS software coupled with the Stanford isotropic bone remodeling model,[12] in order to investigate the process in three-dimensional models of the femur and ORTAN® (Ukraine) prosthesis.

2. Methods

2.1. *Femur model*

For the analysis, a three-dimensional model of the femur was developed based on the results of computed tomography (CT), which allows the creation of three-dimensional models of organs with high accuracy in terms of the shape and properties of soft and bone tissues, giving an almost *in vivo* model. The algorithm for generation of a three-dimensional geometric model of the femur comprised several steps (Fig. 1). For this study, frozen cadaver bones were used. They were scanned at the Dnipropetrovsk State Medical Academy, using an AQUILION RXL 16 (Toshiba Medical Systems) 16-slice CT scanner. DICOM images were obtained with a 0.5 mm slice thickness. Then, CT images of the femur were downloaded for subsequent segmentation of the object. The CT data were processed using MIMICS (Materialise, N.V. — Belgium) software. Segmentation of the images was performed based on the obtained axial projections of the object, using the selection field in the form of a separate mask. The next step comprised the creation of a three-dimensional object on the mask in STL format. Then, the quality of the three-dimensional object was improved by using different functions of surface smoothing. Finally, the assignment of mechanical characteristics of the femur was done by calculating the analytical dependences between the Hounsfield units (HU) obtained from the analysis of computed tomograms (Fig. 1). HU determine the dependence between the radiographic density of the femur tissue, presented in arbitrary units,[17,18] and the actual bone density $-\rho$ (g/cm^3). In our study, the following relationship[19] was used:

$$\rho = 1 + 0.0007185 \cdot \mathrm{HU}. \tag{1}$$

2.2. *Bone remodeling*

The Stanford isotropic bone remodeling model[12] was developed with reference to Beaupre *et al.* The model describes Young's modulus E as a function of the local apparent density ρ:

$$E(\rho) = b(\rho) \times \rho^{\beta(\rho)}, \tag{2}$$

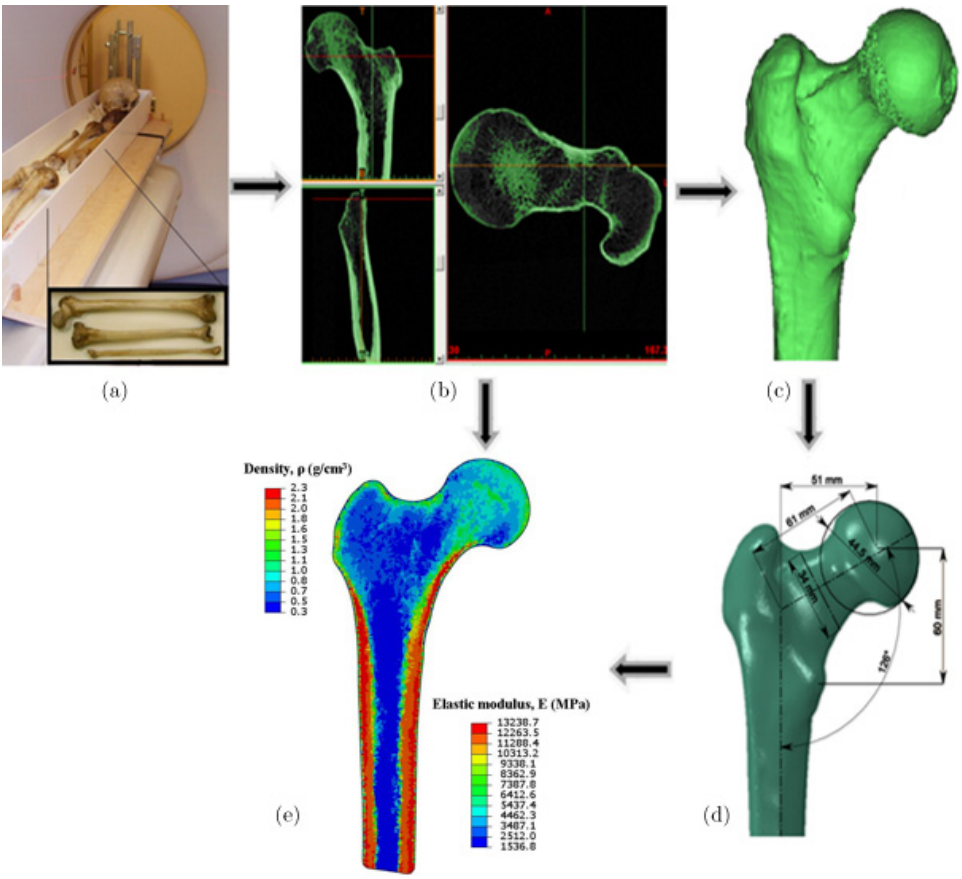

Fig. 1. Three-dimensional model of the femur created from CT images. The main stages of creating the model are: (a) obtaining images of CT of the femur; (b) loading the CT image and segmentation of the object; (c) forming the primary bone geometry; (d) smoothing the model and obtaining solid geometry of the bone; (e) assignment of the mechanical characteristics of the femur.

where $b(\rho)$and $\beta(\rho)$ are auxiliary functions which define the power law function for Young's modulus. Following Jacobs,[12] Stulpner *et al.*,[19]

$$E[MPa] = E(\rho) = \begin{cases} 2014\rho^{2.5} & \text{if } \rho \leq 1.2\,\text{g/cm}^3, \\ 1763\rho^{3.2} & \text{if } \rho > 1.2\,\text{g/cm}^3 \end{cases} \tag{3}$$

is used in this study.

Together with Young's modulus, another material property depending on the value of the local density — Poisson's ratio (ν) — is essential. It is defined as

$$\nu = \nu(\rho) = \begin{cases} 0.2 & \text{if } \rho \leq 1.2\ \text{g/cm}^3, \\ 0.32 & \text{if } \rho > 1.2\ \text{g/cm}^3. \end{cases} \tag{4}$$

The considered bone remodeling model takes into account that bone tissue is stimulated by a so-called daily tissue level stress stimulus, ψ_t, defined as

$$\psi_t = \left(\sum_{\text{days}} n_i \bar{\sigma}^m_{t_i} \right)^{1/m}, \tag{5}$$

where n_i is the daily number of cycles of the load type i and $\bar{\sigma}^m_{t_i}$ is the scalar that quantifies the effective stress in the region of bone tissue associated with the same load, and m is an empirical constant.[12]

Mechanical stimulus is essentially a scalar governing the bone remodeling process and being dependent on the rate of remodeling $\dot{r}$. This rate indicates possible changes in the material properties. In the described model, there are three criteria that determine the change in the properties. First of all, when the mechanical stimulus is greater than the reference value, bone apposition takes place. When the stimulus is smaller than the reference value, bone resorption occurs. Finally, when the stimulus is in a so-called 'dead zone', there is no change in the mechanical properties, and thus this stimulus is in a bone equilibrium state. The rate of remodeling can be described as

$$\dot{r} = \begin{cases} c[(\psi_t - (\psi^*_t - w)] & \text{if } \psi_t < (\psi^*_t - w), \\ 0 & \text{if } (\psi^*_t - w) < \psi_t < (\psi^*_t + w), \\ c[(\psi_t - (\psi^*_t + w)] & \text{if } \psi_t > (\psi^*_t + w). \end{cases} \tag{6}$$

In this case, ψ^*_t is the reference daily stress stimulus and defines a function where there is no change in the material properties (the so-called 'dead zone'), c is the slope of the bone remodeling curve, and w is the half-length of the dead zone.

For an apparent density ρ the effective scalar stress can be related to the material continuum stress level, termed the apparent stress $\bar{\sigma}(\rho)$:

$$\bar{\sigma}(\rho) = \left(\frac{\rho}{\rho_c} \right)^2 \bar{\sigma}_t, \tag{7}$$

where ρ_c stands for the maximum value of the density for the cortical bone. The apparent stress is determined by

$$\bar{\sigma}_i(\rho) = \sqrt{2E(\rho)U_i(\rho)}, \tag{8}$$

where $E(\rho)$ is Young's modulus and $U_i(\rho)$ is the strain density energy, which is calculated as $U_i = U_i(\rho) = \frac{1}{2}\varepsilon_i : C(\rho) : \varepsilon_i$, where ε_i is the stain tensor and $C(\rho)$ is the elastic constant tensor.

The specific surface area, S_v, can be expressed in terms of the apparent density ρ.[20] This parameter is a scalar that quantifies the internal surface of tissue per density of its volume.

The specific surface is obtained directly from a tomography and can be written as

$$S_v = -0.07 + 8.1\rho - 7.2\rho^2 + 5.1\rho^3 - 2.1\rho^4 + 0.23\rho^5. \tag{9}$$

Finally, the rate of density evolution, $\dot{\rho}$, can be determined as

$$\dot{\rho} = S_v \dot{r} \rho_c. \tag{10}$$

The finite element analysis is implemented using ABAQUS software (version 6.14, Dassault Systems, 2015). The remodeling process is divided into many time steps (Fig. 2). ABAQUS allows users to include custom subroutines, written in Fortran, to enhance the capabilities of analysis. In our work, a 'SDVINI' subroutine was used to import the initial density distribution obtained from a CT of the femur. Within each time step, the bone remodeling is embedded in the finite element analysis. In the element-based approach, the bone remodeling process is implemented through a 'UMAT' user-subroutine. As illustrated in the bone remodeling algorithm (Fig. 2), for the next steps (iterations), new properties of each element are calculated based on the concentration of old and new bone remaining/produced inside the element. In this study, each remodeling period was chosen to denote one day. In total, 730 iterations were performed for every finite element model, simulating the remodeling period of two years.

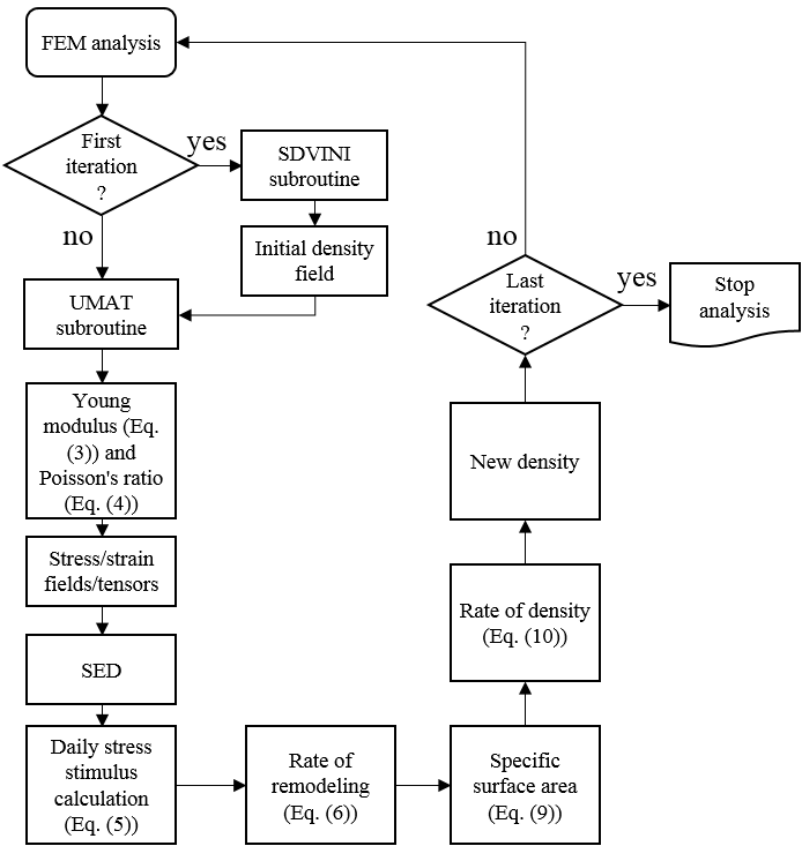

Fig. 2. Block diagram of the isotropic Stanford model algorithm.

2.3. *Models and boundary conditions*

In this work, the size and the shape of the ORTAN® (Ukraine) femoral component is used. The physical properties of stainless steel (316L), having a Young's modulus $E = 200$ GPa and Poisson's ratio of 0.3, have been chosen to describe the material of the femoral component of the hip endoprosthesis. To investigate the impact of cement mantle thickness, five different models were created to represent different thickness of the cement mantle (1, 2, 3, 4 and 5 mm) between the femoral bone and the implant. We change the stem geometry size in order to obtain five different thickness of cement mantle (for size 1 thickness of cement mantle was modeled equal to 5 mm, for size 2–4 mm, for size 3–3 mm, for size 4–2 mm, and for size 5–1 mm (Fig. 3)). The models enable the study of the case when rasping of the medullary canal is performed too aggressively in the process of bed preparation for introduction of the bone cement and implant stem, which results in thinning of the bones. It is important to mention that we use the 5 mm thickness only for a numerical evaluation and to study the process.

Young's modulus of the cement was specified as 2.5 GPa and Poisson's ratio was 0.29. In the interface between hip endoprosthesis and cement, we model it using a surface-to-surface contact algorithm (in Abaqus software) with the Coulomb stick-slip model of friction, with a friction coefficient equal to 0.25; this simulates the surface finish for the stem. Contact loads, acting from the acetabulum to the head of the endoprosthesis, are calculated according to experimental observations performed by Bergman *et al.*[21] on a patient of 80 kg weight. In addition, forces acting on the surface of the bone in places of attachment of muscles have been taken into

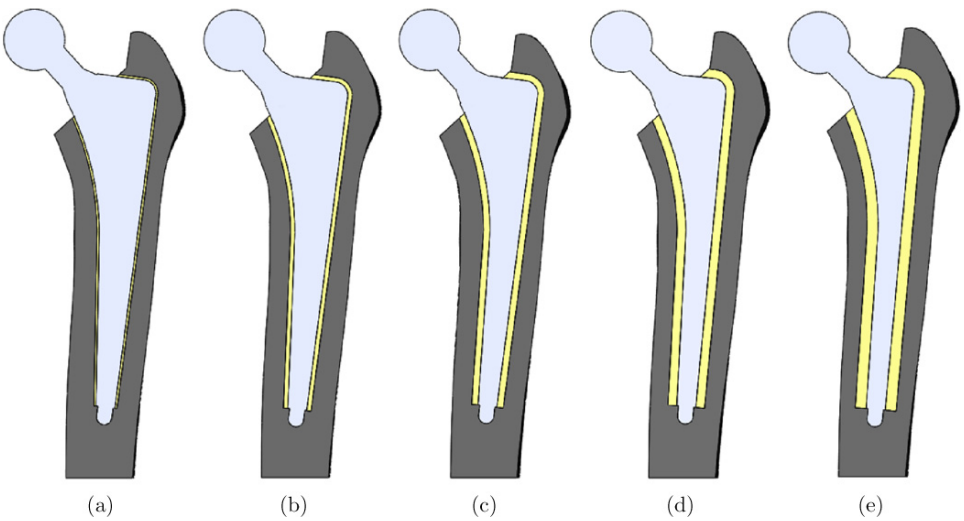

Fig. 3. Geometric models used in the study, characterized with the mantle cement thickness of (a) 1, (b) 2, (c) 3, (d), 4 and (e) 5 mm, respectively.

account.[22] We considered a single-load case comprising a force on the femoral head and another on the greater trochanter. This provides a bone deposition along the main stress direction, which naturally results in orthotropic trabecular orientations.[16]The FE bone-cement-implant system models used in this study comprise 1,100,123 3D solid four-node tetrahedral elements. For all elements of the system, the length of the edge of mesh elements equals 1 mm.

3. Results

Using the bone remodeling theory,[12] changes in bone density (two years after prosthesis implantation) were predicted for the cemented stem fixation. Bone density distributions obtained due to change in the cement thicknesses are shown in Fig. 4. One can clearly observe the bone resorption process, mainly in the proximal portion of the femur due to stress shielding. The use of the cement mantle helps to maintain bone density over the bone-cement-endoprosthesis interface and in the proximal region, which is the most affected region due to the bone resorption process, as shown in Figs. 4(b)–4(f). The load transmission level is improved for the host bone in the case of a relatively thick cement mantle (4 mm and 5 mm) and a reduction of stem size. The combination of these two factors helps to decrease the difference between bone and prosthesis stiffness. In the distal portion, stress concentration points are clearly observed, which provides a high-level bone formation. This works in a similar manner to bone-prosthesis anchoring due to compressive load application and bone resorption on the proximal region. The results also show that there is a decrease in bone resorption on proximal and distal regions for cement mantle thicknesses of 3, 4 and 5 mm (Figs. 4(d)–4(f)).[23,24] Using a very small thickness (less than 1 mm) provides a situation similar to a noncemented prosthesis, where there is a large difference between the stiffness of the bone and prosthesis, and

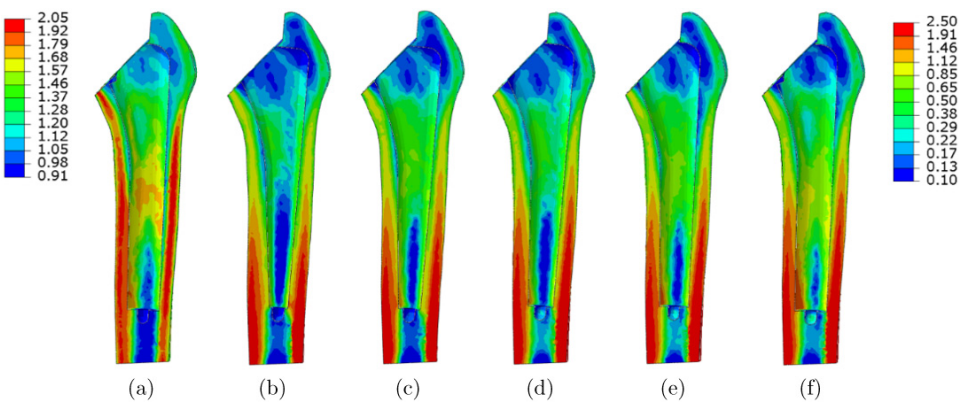

Fig. 4. Bone density (in g/cm^3) distribution for the femur two years after hip replacement. Initial (a) and final models of cement mantle thickness of (b) 1, (c) 2, (d) 3, (e) 4 and (f) 5 mm.

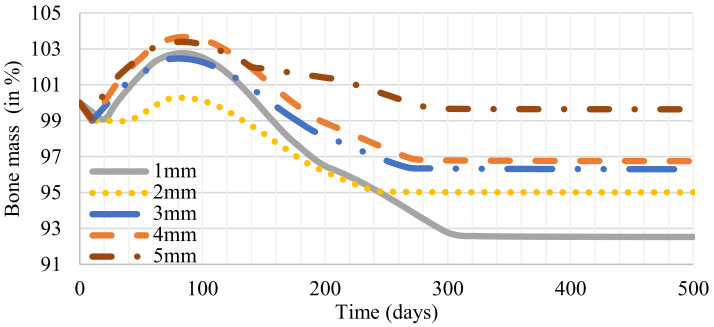

Fig. 5. Total bone mass variation with time for different cement mantle thicknesses two years after hip replacement.

provides high-level stress shielding in the proximal region. The total bone mass variation over the simulation time is shown in Fig. 5 for different cement mantle thicknesses. It can be seen that thicker cement mantles (i.e., 4 mm and 5 mm) helps to maintain the bone in the medial interface region and lead to less resorption in total bone density.

In Fig. 6, we report the distributions and values of the equivalent stress for the cement mantle. The curve number corresponds to the thickness of the cement mantle in mm. In the cement mantle, tensile stresses arise from the lateral side while

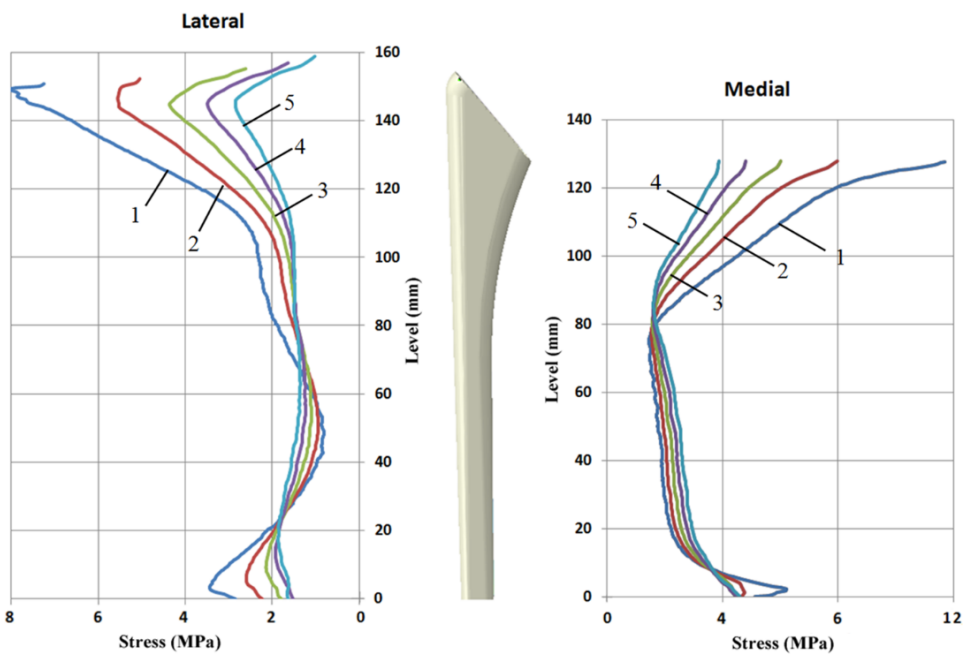

Fig. 6. Distribution of maximum equivalent stress on medial and lateral sides of cement mantle for different thicknesses of cement mantle.

compressive stresses from the medial one (Fig. 6). Cement mantle maximum compressive stresses are concentrated in the proximal zone of Adam's arc of the femur. Comparing the bone cement fatigue limit, being equal to 10 MPa,[25,26] with the stresses in the cement mantle, it has been noted that the environment has no destructive influence on the functioning of the implant when the thickness of the cement mantle equals at least 2 mm. We note that changes in the thickness of the cement mantle affect the magnitude of stresses arising in the proximal zone of the endoprosthesis fixation and more on the proximal portion of the femur than the distal one (Fig. 6).

The stress–strain state of the stem is defined by a combination of the bending moment in the frontal plane and the compression forces in the axial direction, with essential predominance of the first. On the lateral side of the stem and the neck taper, normal longitudinal tension appears while on the medial side — compression. Thus, the absolute value of tension at the same level of the stem is slightly smaller than that of compression. The maximum stress value is observed on the lateral side, at the level of the neck and taper for fixing the head of the femoral component. Changes in thickness of the cement mantle have no considerable effect on the stress state of the implant stem. Calculation results show that the maximum tension does not exceed the yield strength of the material, and all elements of the system operate in the elastic deformation region. Note also that tension in the implant is below the fatigue limit (being the resistance to fatigue under cyclic load), which provides a sufficient margin of safety for the endoprosthesis stem.[27]

4. Discussion

This study aimed to evaluate a few cases of different thickness of cement mantle around a total femoral endoprosthesis to investigate the impact of cement mantle thickness on the stress and bone density distributions and the bone-cement-endoprosthesis interface.

The conclusion can be drawn that stress on the lateral and medial sides of the cement mantle decreases following an increase in cement mantle thickness. This phenomenon is particularly observed in the proximal region of the endoprosthesis, which is more prone to bone resorption due to inserted implants of higher stiffness. With the increase in cement mantle thickness, the bone-cement-endoprosthesis system becomes stiffer than for thinner mantles. Our results confirm experimental verification of the results of the finite-element modeling presented in the work of Estok *et al.*,[28] in which a 45–55% decrease in peak distal cement strains was obtained by increasing the cement mantle thickness from 2.5 mm to 5 mm, keeping a constant prosthesis diameter. A subsequent computational study by Lee *et al.*[29] showed a 45% reduction in peak tensile cement stresses when cement mantle thickness was changed from 2 mm to 5 mm by means of reducing the prosthesis diameter. Also, Fisher *et al.*[30] conducted an experiment with two different sizes of cobalt–chromium stems and found in the case of raising the cement mantle

thickness from 2.4 mm to 3.7 mm, substantial strain reduction in the distal cement (40–49%) resulted.

An important study with a similar methodology and very similar conclusions was conducted by Perez *et al.*,[31] who investigated bone adaptions around a resurfacing cemented prosthesis. The authors evaluated bone behavior for different cement mantle thicknesses and interface conditions. They showed that a very thin cement mantle is detrimental for bone, which produces meaningful bone resorption.

With respect to bone density distribution, higher cement mantle thicknesses help maintain the bone, causing a low level of bone resorption in critical regions such as proximal and medial portions of the interface. High levels of resorption in these regions can cause aseptic loosening of the implant, which, in turn, raises the need for another surgical procedure.

In order to select the most appropriate size for this study's approach, we considered two aspects. The first involved stress distribution along the cement mantle. When we compare these values with cement bone fatigue limits of between 8–10 MPa, the best choice would be a thick mantle, since it provides a stress distribution that does not reach the material property limits. The second aspect considered is bone density distribution. Thick cement mantles help to decrease the stiffness difference value between bone and endoprosthesis. This increase in thickness improves load transmission in the proximal portion of the femur, which is the main area for bone resorption caused by stress shielding. However, the choice of a large and thick (more than 4 mm) cement mantle cannot be implemented due to the size of femoral cavity in which the component is to be inserted. Thus, an intermediate thickness (i.e., 3 mm) should be chosen, since it would be capable of ensuring a considerable stress distribution and does not cause significant changes in bone density distribution two years after component installation. Another aspect of note is that thicker cement mantles increase polymerization temperatures at the interface, which leads to thermal necrosis.[17] The selected cement mantle size is in agreement with results found in the literature. Fisher *et al.*[30] demonstrated that a thickness of 2–3 mm might provide a more favorable situation for the system than a thinner mantle. Ramanikara *et al.*[23] suggested an optimum thickness of around 3–5 mm. Cristofolini *et al.*[24] indicate that a 3-mm thickness shows adequate performance. Thus, an ideal cement mantle which would most likely be acceptable to the orthopedic community should exhibit a thickness of 2–4 mm.[32]

Regarding the efficiency of the FEM, some limitations should be noted. First, the model considers isotropic material properties of the femur which may not reflect the *in vivo* situation. Also, simple load conditions are applied, with loads being used that occur in a gait step, and other situations are not considered by the model used in this study. Another limitation concerns the cement mantle, where we simulate it with a uniform thickness; however, this does not adequately reflect real situations. Another issue of note is that the bone remodeling model used corresponds to the well-known Stanford model by Jacobs and Beaupre, in terms of its isotropic version. This Stanford model is not new; however, it provides bone formation along the main

stress directions, which naturally results in orthotropic trabecular orientations and follows Wolff assumptions. Thus, the method, if coupled with the bone remodeling model, enables the determination of results that can be qualitatively compared with clinical ones.

Acknowledgment

This work has been supported by the National Science Centre of Poland under the grant OPUS 9 No. 2015/17/B/ST8/01700 for the years 2016–2018.

References

1. Doblaré M, García JM, Application of an anisotropic bone-remodeling model based on a damage-repair theory to the analysis of the proximal femur before and after total hip replacement, *J Biomech* **34**:1157–1170, 2001.
2. García JM, Doblaré M, Cegoñino J, Bone remodeling simulation: A tool for implant design, *Comput Mater Sci* **25**:100–114, 2002.
3. Lemaire V, Tobin FL, Greller, LD, Cho CR, Suva LJ, Modeling the interactions between osteoblast and osteoclast activities in bone remodeling, *J Theor Biol* **229**:293–309, 2004.
4. Jordão P, Bahute A, Fountoura U, Marques P, Femoral cementing techniques, *Revista Portuguesa de Ortopedia e Traumatologia* **21**:473–478, 2013.
5. Bhambri SK, Gilbertson LN, Micromechanisms of fatigue crack initiation and propagation in bone cements. *J Biomed Mater Res* **29**:233–237, 1995.
6. Kroell A, Beaulé P, Krismer M, Behensky H, Stoeckl B, Biedermann R, Aseptic stem loosening in primary THA: Migration analysis of cemented and cementless fixation, *J Int Orthopaedics* **33**:1501–1505, 2009.
7. Meding JB, Herbst SA, Keating EM, Faris PM, Ritter MA, Radiographic analysis of a cemented titanium alloy femoral component, *Clin Orthop Relat Res* **334**:184–189, 1997.
8. Huddleston HD, Femoral lysis after cemented hip arthroplasty, *J Arthroplasty* **3**:285–297, 1988.
9. Anthony PP, Gie GA, Howie CR, Ling RS, Localised endosteal bone lysis in relation to the femoral components of cemented total hip arthroplasties, *J Bone Joint Surg Br* **72**:971–979, 1990.
10. Beaupré GS, Orr TE, Carter DR, An approach for time-dependent bone modeling and remodeling-application: A preliminary remodeling simulation, *J Orthop Res* **8**:651–661, 1990.
11. Weinans H, Huiskes R, Grootenboer HJ, Effects of material properties of femoral hip components on bone remodeling, *J Orthop Res* **10**:845–853, 1992.
12. Jacobs CR, Numerical simulation of bone adaptation to mechanical loading, PhD thesis, Stanford Universiy, 1994.
13. Jacobs CR, Simo JC, Beaupré GS, Carter DR, Adaptive bone remodeling incorporating simultaneous density and anisotropy considerations, *J Biomech* **30**:603–613, 1997.
14. McNamara LM, Prendergast PJ, Bone remodeling algorithms incorporating both strain and microdamage stimuli, *J Biomech* **40**:1381–1391, 2007.
15. Mercuri EGF, Daniel AL, Machado RD, Hecke MB, Application of a multi-scale mechanobiological model for bone remodeling, *J Med Imaging Health Inf* **4**:1–5, 2014.

16. Herrera A, Rebollo S, Ibalz E, Mateo J, Gabarre S, Gracia l, Mid-term study of bone remodeling after femoral cemented stem implantation: Comparison between DXA and finite element simulation, *J Arthroplasty* **29**:90–100, 2014.
17. Cann C, Quantitative CT for determination of bone mineral density: A review, *J Radiol* **166**:509–522, 1988.
18. Peng L, Bai J, Zeng X, Zhou Y, Comparison of isotropic and orthotropic material property assignments on femoral finite element models under two loading conditions, *J Med Eng Phys* **28**:227–233, 2007.
19. Stulpner MA, Reddy BD, Starke GR, Spirakistz A, A three-dimensional finite analysis of adaptive remodeling in the proximal femur, *J Biomech* **30**:1063–1066, 1997.
20. Corso LL, Application of optimization procedures and bone remodeling in a simulation and analysis of biomechanics problems, MSc. Degree Thesis, Federal University of Rio Grande do Sul, 2006.
21. Bergmann G, Deuretzbacher G, Heller M, Graichen F, Rohlmann A, Strauss J, Duda GN, Hip contact forces and gait patterns from routine activities, *J Biomech* **34**:859–871, 2001.
22. Heller MO, Bergmann G, Kassi JP, Claes L, Haas NP, Duda GN, Determination of muscle loading at the hip joint for use in pre-clinical testing, *J Biomech* **38**:1155–1163, 2005.
23. Ramaniraka NA, Rakotomanana LR, Leyraz, PF, The fixation of the cemented femoral component, *Bone Joint Surg* **82**:297–303, 2000.
24. Cristofolini L, Erani P, Savigni P, Grupp T, Thies O, Viceconte M, Increased long-term failure risk associated with excessively thin cement mantle in cemented hip arthroplasty: A comparative in vitro study, *Clin Biomech* **22**:410–421, 2007.
25. Baleani M, Cristofolini L, Minari C, Toni A, Fatigue strength of PMMA bone cement mixed with gentamicin and barium sulphate vs pure PMMA, *Proc Inst Mech Eng H* **217**:9–12, 2003.
26. Bialoblocka-Juszczyk E, Baleani M, Cristofolini L, Viceconti M, Fracture properties of an acrylic bone cement, *Acta Bioeng Biomech* **10**:21–26, 2008.
27. Maruyama N, Mori D, Hiromoto S, Kanazawa K, Nakamura M, Fatigue strength of 316L-type stainless steel in simulated body fluids, *J Corros Sci* **53**:2222–2227, 2011.
28. Estok DM, Harrigan TP, Harris WH, Finite element analysis of cement strains at the tip of an idealized cemented femoral component, *Trans ORS* **16**:504, 1991.
29. Lee IY, Skinner HB, Keyak JH, Effects of variation of prosthesis size on cement stress at the tip of a femoral implant, *J Biomed Mater Res* **28**:1055–1066, 1994.
30. Fisher DA, Tsang AC, Paydar N, Milionis S, Turner CH, Cement-mantle thickness affects cement strains in total hip replacement, *J Biomech* **30**:1173–1177, 1997.
31. Pérez MA, Vendittoli PA, Lavigne M, Nuño N, Bone remodeling in the resurfaced femoral head: Effect of cement mantle thickness and interface characteristics, *Med Eng Phys.* **36**:185–195, 2014.
32. Garcia FL, Sugo AT, Picado CHF, Radiographic grading of femoral stem cementation in hip arthroplasty, *Acta Ortopédica Brasileira*, **21**:30–33, 2013.